actions of HCN with ions such as $C_n^+$, $C_nH^+$, and $C_nCN^+$ to produce the adducts are quite likely.

## Conclusions

The study of HCN reactions with small positive carbon cluster ions has given a number of new and interesting results.

(1) The reactivity of carbon clusters and their HCN reaction products follows a simple empirical rule correlated to the radical/nonradical nature of the ion.

(2) The variations in product branching ratios within a homologous series of reactions can be predicted by energetic considerations alone.

(3) The proposed mechanism for reaction of the linear cluster ions at the carbene sites is only partially correct. The first HCN appears to add covalently at the carbene, but the second HCN preferentially associates with the ion, most likely by hydrogen bonding to the first HCN fragment in the ion.

(4) In addition to $C_7^+$, the $n = 8$ and 9 clusters are also present as two different structural isomers, which the results indicate are linear and cyclic. There is no compelling evidence for the existence of other cyclic isomers such as $C_4^+$.

(5) The $C_7^+$ cluster behaves in an anomalous fashion, which we interpret in part as due to the isomerization of the cyclic form during reaction.

(6) Positive carbon clusters undergo efficient radiative association reactions with HCN. This observation has important implications for interstellar chemistry.

**Acknowledgment.** We thank V. Anicich (JPL), B. Dunlap, M. Hanratty, and J. Rice for helpful discussions.

**Registry No.** HCN, 74-90-8.

# Fundamental Studies of the Energetics and Dynamics of Ligand Dissociation and Exchange Processes at Transition-Metal Centers in the Gas Phase: $Mn(CO)_x^+$, $x = 1–6$

**David V. Dearden,[†] Kathleen Hayashibara,[†] J. L. Beauchamp,*[,†] Nicholas J. Kirchner,[‡] Petra A. M. van Koppen,[‡] and Michael T. Bowers*[,‡]**

*Contribution No. 7850 from the Arthur Amos Noyes Laboratory of Chemical Physics, California Institute of Technology, Pasadena, California 91125, and Department of Chemistry, University of California, Santa Barbara, California 93106.* *Received September 14, 1988*

**Abstract:** A significant change in spin multiplicity results from sequential addition of CO to $Mn^+$ ($^7S$) to form $Mn(CO)_6^+$ ($^1A_{1g}$). To explore the possible effects of changes in spin multiplicity on the dynamics of ligand dissociation and exchange processes at transition-metal centers in the gas phase, we have measured labeled CO exchange rates ($x = 1–6$) and kinetic energy release distributions (KERDs) for metastable decomposition by loss of CO ($x = 2–6$) for $Mn(CO)_x^+$. With the exception of the coordinatively saturated species $Mn(CO)_6^+$, for which no ligand exchange is observed, the CO exchange rates are within an order of magnitude of collision limited in all cases. All KERDS were statistical, indicating no barrier in the CO-loss exit channel. These results are discussed in terms of the requirements for spin conservation in ligand exchange reactions. Quantitative analysis of statistical KERDs requires a knowledge of the internal energy of the decomposing species, which in the present experiment are formed by electron impact with a broad range of internal energies. We demonstrate that the temporal constraints of the experiment select metastables with a particular range of internal energies, which can be bracketed using RRKM theory, enabling the KERDs to be modeled using phase space theory. Individual $D_0^0(Mn(CO)_{x-1}^+–CO)$ (kcal/mol) values were determined by fitting the phase space calculations to the experimental KERDs: $x = 6$, $32 \pm 5$; $x = 5$, $16 \pm 3$; $x = 4$, $20 \pm 3$; $x = 3$, $31 \pm 6$; $x = 2$, $<25$; $x = 1$, $>7$.

In a recent series of studies on the addition rates of CO to coordinatively unsaturated, neutral metal carbonyls, spin conservation was used to explain the large variations in the rates for reaction 1 among members of the $Fe(CO)_x$ system. For $x = 4$,

$$M(CO)_x + CO \rightarrow M(CO)_{x+1} \quad (1)$$

the rate was 2.5 orders of magnitude slower than that for $x = 3$ or $x = 2$, which have rates within 1 order of magnitude of the collision rate.[1,2] Since $Fe(CO)_5$ has a singlet ground state while $Fe(CO)_4$ is known from magnetic circular dichroism studies to be a triplet,[3] the recombination rates were taken to be a reflection of the spin-forbidden nature of CO addition to $Fe(CO)_4$, while it was assumed that CO addition to $Fe(CO)_2$ and to $Fe(CO)_3$ are spin-allowed processes. Subsequent studies on $Cr(CO)_x$ ($x = 5–2$)[4,5] and $Co(CO)_x$ ($x = 1–3$)[6] found that the CO recombination rates were all fast, leading to the suggestion that all of these recombination reactions proceed with spin conservation. A natural question arising from this work is whether or not the spin conservation requirement for rapid reaction is general.

* Authors to whom correspondence should be addressed.
[†] California Institute of Technology.
[‡] University of California.

(1) Ouderkirk, A. J.; Wermer, P.; Schultz, N. L.; Weitz, E. *J. Am. Chem. Soc.* **1983**, *105*, 3354–3355.
(2) Seder, T. A.; Ouderkirk, A. J.; Weitz, E. *J. Chem. Phys.* **1986**, *85*, 1977–1986.
(3) Barton, T. J.; Grinter, R.; Thomson, A. J.; Davies, B.; Poliakoff, M. *J. Chem. Soc., Chem. Commun.* **1977**, 841–842.
(4) (a) Fletcher, T. R.; Rosenfeld, R. N. *J. Am. Chem. Soc.* **1985**, *107*, 2203–2212. (b) Fletcher, T. R.; Rosenfeld, R. N. *J. Am. Chem. Soc.* **1986**, *108*, 1686–1688. (c) Fletcher, T. R.; Rosenfeld, R. N. *J. Am. Chem. Soc.* **1988**, *110*, 2097–2101.
(5) (a) Seder, T. A.; Church, S. P.; Ouderkirk, A. J.; Weitz, E. *J. Am. Chem. Soc.* **1985**, *107*, 1432–1433. (b) Seder, T. A.; Church, S. P.; Weitz, E. *J. Am. Chem. Soc.* **1986**, *108*, 4721–4728.
(6) Rayner, D. M.; Nazran, A. S.; Drouin, M.; Hackett, P. A. *J. Phys. Chem.* **1986**, *90*, 2882–2888.

0002-7863/89/1511-2401$01.50/0 

An equally interesting area is that of bond energetics for metal carbonyls, especially where the potential exists for determining individual, rather than average, M–CO bond energies. Despite the fact that stable transition-metal carbonyl compounds have been known for the better part of a century, the bonding in these compounds remains a subject of discussion. Such interest is understandable in light of such facts that the basic structures of simple metal carbonyl fragments serve as building blocks for assembling large, polynuclear compounds, that metal carbonyl species are potentially important in a number of catalytic processes, and that the theoretical description of bonding in such species remains a challenge. Considerable data exist for coordinatively saturated metal carbonyls, but relatively little is available for the coordinatively unsaturated fragments. Photochemical and kinetic[7] methods, as well as photodetachment from anions,[8,9] have been used to obtain information on neutral species, while appearance potentials have been measured for a few series of metal carbonyl fragment ions.[10,11] Further information in this area is valuable for understanding bonding trends in homologous series as well as periodic relationships.

The $Mn(CO)_x^+$ ($x = 0$–6) system presents an opportunity to study both the role of spin conservation in "simple" ligand exchange processes and bond energetics. Since this is a $d^6$ system, a variety of spin states are possible. $Mn^+$ has a $^7S$ ground state[12] while the $Mn(CO)_6^+$ ground state is $^1A_{1g}$.[13,14] Although the ground spin states for intermediate members of the series are unknown, it is likely that more than one spin state is exhibited among the ground states of the $Mn(CO)_x^+$ series, leading to the anticipation of slow rates for reactions involving changes in spin multiplicity at the metal center. These ions are isoelectronic with the well-studied $Cr(CO)_x$ system,[4,5] offering a chance to compare bonding in an ionic system with that of a series of coordinatively unsaturated neutrals.

To probe the energetics and ligand dissociation dynamics of the $Mn(CO)_x^+$ system, we report the results of two different experiments. In the first, CO exchange rates are examined by observing the incorporation of $^{13}CO$ into the $Mn(CO)_x^+$ ions. This experiment is closely analogous to the CO recombination experiments with coordinatively unsaturated, neutral metal carbonyls noted above, since in order to exchange CO, the $Mn(CO)_x^+$ must undergo CO addition. In the neutral case the recombination product is collisionally stabilized, while in the exchange experiments, carried out at low pressure, the adduct is not stabilized and loss of any CO but the label results in exchange. The aim of these experiments is to detect spin-forbidden processes in a manner analogous to that used for the neutral studies noted above.

In the second experiment, the potential surfaces for ligand loss are probed by measuring the kinetic energy released when metastable $[Mn(CO)_x^+]^*$ decomposes through CO loss. If decomposition occurs on a "Type 1" surface (where there is no barrier to the reverse CO addition reaction), the kinetic energy release is expected to be in accord with the predictions of statistical theory. If a "Type II" surface is involved, with a barrier in the exit channel, a broad range of kinetic energies peaking away from zero is expected.[15]

A major advantage of the kinetic energy release experiments is the possibility of extracting quantitative information on the energetics of the decomposition, even when the metastable ions are not prepared with well-defined internal energies. A method for obtaining this information by modeling the experimental results using statistical theory is described, and the technique is applied to determine individual $Mn^+$–CO bond energies for members of the $Mn(CO)_x^+$ system.

**Table I.** Typical Fragment Intensities 150 ms after Ionization

| $Mn(CO)_5COCF_3$ (electron energy 15 eV) | | $Mn(CO)_5COCH_3$ (electron energy 22 eV) | |
|---|---|---|---|
| $m/z$ | relative intensity | $m/z$ | relative intensity |
| 111.5 | 5.0 | 55.0 | 5.9 |
| 124.0 | 8.3 | 70.0 | 36.5 |
| 139.0 | 6.0 | 83.0 | 14.1 |
| 152.0 | 6.9 | 98.0 | 19.7 |
| 154.0 | 3.3 | 111.0 | 21.9 |
| 167.0 | 7.2 | 126.0 | 13.7 |
| 180.0 | 5.1 | 137.0 | 6.5 |
| 182.0 | 8.7 | 139.0 | 30.8 |
| 195.0 | 20.3 | 144.0 | 5.6 |
| 210.0 | 3.2 | 154.0 | 16.6 |
| 223.0 | 100.0 | 164.5 | 10.0 |
| 224.0 | 7.1 | 167.0 | 59.8 |
| 264.0 | 7.3 | 179.0 | 5.8 |
| | | 182.0 | 73.3 |
| | | 191.5 | 8.8 |
| | | 195.0 | 39.7 |
| | | 196.0 | 7.5 |
| | | 206.5 | 6.8 |
| | | 210.0 | 100.0 |
| | | 211.0 | 7.8 |
| | | 224.0 | 45.0 |
| | | 232.5 | 11.8 |
| | | 237.0 | 86.1 |

## Experimental Section

Exchange experiments using $^{13}CO$ were performed with a Fourier transform ion cyclotron resonance spectrometer equipped with a 1-in. cubic cell and a data acquisition system supplied by Ion Spec Corp. $Mn(CO)_x^+$ ions were produced by 15–35-eV electron impact on either $Mn(CO)_5COCH_3$ ($x = 1$–5) or $Mn(CO)_5COCF_3$ ($x = 1$–6). Typical fragment intensities 150 ms after the end of the electron beam pulse are given for these compounds in Table I. Electron energies were adjusted to maximize the intensity of the ion of interest. In some cases collision-induced dissociation was performed using $^{13}CO$ as the collision gas, in order to enhance the population of fragment ions. With these methods of ion production, it is expected that the resulting species are produced with a broad range of internal energies. The $Mn(CO)_x^+$ ions were isolated using sweep-out pulses and allowed to react with $(0.5$–$1.3) \times 10^{-6}$ Torr $^{13}CO$ for up to 1 s. Decay of the $Mn(CO)_x^+$ signal, as well as growth of signal due to singly and multiply $^{13}CO$-substituted products, was followed as a function of time. Pressures were measured using a Schultz–Phelps ionization gauge calibrated against a MKS Baratron capacitance manometer.

Rate constants for $^{13}CO$ exchange reactions were determined by analysis of the decay of $Mn(CO)_x^+$ in cases where side reactions (primarily charge transfer) were not important. Where side reactions were significant, the constants were determined by plotting $\ln (I/I_0)$ versus time, where $I$ and $I_0$ are the absolute signal intensities in the presence and absence of $^{13}CO$, respectively.[16] The reported rate constants are the average and standard deviation of several measurements. It is important to note that the same results, within experimental error, were obtained using $Mn(CO)_5COCH_3$ to generate $Mn(CO)_x^+$ ions as were obtained using $Mn(CO)_5COCF_3$ and that the same results were obtained both in the presence and absence of side reactions.

Kinetic energy release experiments for metastable decomposition, photodissociation, and CID experiments were performed on a VG Industries ZAB-2F double-focusing, reverse geometry mass spectrometer with a home-built temperature- and pressure-variable electron impact source. The techniques used in metastable decomposition[17] and photodissociation studies[18] have been described in detail elsewhere. Briefly, samples of $Mn(CO)_5COCH_3$ or $Mn(CO)_5COCF_3$ were heated to ap-

(7) Graham, J. R.; Angelici, R. J. *Inorg. Chem.* **1967**, *6*, 2082–2085.
(8) Engelking, P. C.; Lineberger, W. C. *J. Am. Chem. Soc.* **1979**, *101*, 5569–5573.
(9) Stevens, A. E.; Feigerle, C. S.; Lineberger, W. C. *J. Am. Chem. Soc.* **1982**, *104*, 5026–5031.
(10) Michels, G. D.; Flesch, G. D.; Svec, H. J. *Inorg. Chem.* **1980**, *19*, 479–485.
(11) Simoes, J. A. M.; Schultz, J. C.; Beauchamp, J. L. *Organometallics* **1985**, *4*, 1238–1242.
(12) Sugar, J.; Corliss, C. *J. Phys. Chem. Ref. Data* **1985**, *14*, 351–363.
(13) Beach, N. A.; Gray, H. B. *J. Am. Chem. Soc.* **1968**, *90*, 5713–5721.
(14) Burdett, J. K. *J. Chem. Soc., Faraday Trans. 2* **1974**, *70*, 1599–1693.
(15) Hanratty, M. A.; Beauchamp, J. L.; Illies, A. J.; van Koppen, P. A. M.; Bowers, M. T. *J. Am. Chem. Soc.* **1988**, *110*, 1–14.
(16) Stevens, A. E.; Beauchamp, J. L. *Chem. Phys. Lett.* **1981**, *78*, 291–295.
(17) Jarrold, M. F.; Illies, A. J.; Bowers, M. T. *Chem. Phys.* **1982**, *65*, 19.
(18) (a) Jarrold, M. F.; Illies, A. J.; Bowers, M. T. *J. Chem. Phys.* **1983**, *79*, 6086. (b) Jarrold, M. F.; Illies, A. J.; Bowers, M. T. *J. Chem. Phys.* **1984**, *81*, 214–221. (c) Jarrold, M. F.; Illies, A. J.; Bowers, M. T. *J. Chem. Phys.* **1985**, *82*, 1832.

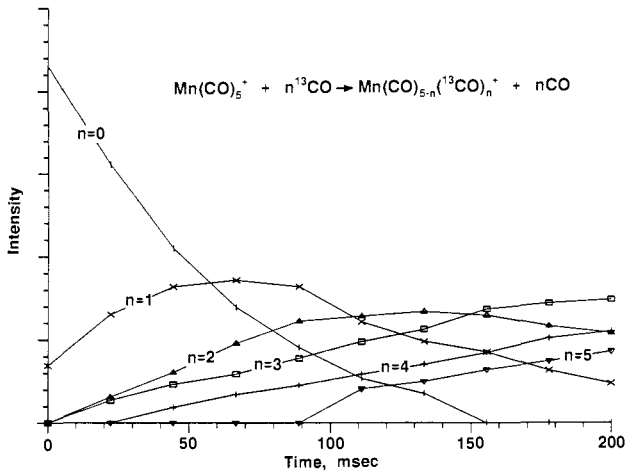


**Figure 1.** Results of FTICR $^{13}CO$ exchange experiment for $Mn(CO)_5^+$. $Mn(CO)_5^+$ was generated by collision-induced dissociation (CID) of $Mn(CO)_6^+$ produced from electron impact on $Mn(CO)_5COCF_3$. $P_{CO}$ = $1 \times 10^{-5}$ Torr. Signal intensities normalized such that $\sum I(Mn(CO)_{5-n}(^{13}CO)_n^+) = 1$ for $n$ = 0–5. The zero on the time scale corresponds to the end of the excitation pulse used for CID.

proximately 50 °C and introduced into the source through a leak valve, with pressures in the source of approximately 10 mTorr as determined by a Baratron capacitance manometer. Typically, $Mn(CO)_x^+$ ($x$ = 1–6) ions were produced at electron energies of approximately 300 eV, with the energy varied to maximize ion beam intensity. Again, the resulting ions are expected to exhibit a broad range of internal energies. In metastable studies, the energy resolution of the beam was always better than 2-eV fwhm and typically was better than 1 eV, while for photodissociation studies the resolution was approximately 6-eV fwhm. The identity of the $Mn(CO)_x^+$ ions was verified by CID. The ions were extracted from the source and accelerated to 8 keV, after which they passed through a magnetic sector for mass analysis where the ion of interest was selected. Next the ions entered the second field-free region where metastable decomposition (or collision with He for CID experiments) took place. Photodissociation was performed by crossing the mass-selected ion beam at its secondary focal point in the second field-free region with the output of an $Ar^+$ ion laser (Coherent, Innova 20) operating on the 514-nm line, after passage of the laser beam through a polarization rotator (Spectra Physics, 310A). Fragment ions produced in the second field-free region were energy analyzed in an electric sector and detected using pulse counting techniques. The background pressure in the second field-free region was less than $1 \times 10^{-9}$ Torr for metastable and photodissociation studies. For CID experiments He was added to the collision cell until an indicated pressure of $(2-3) \times 10^{-8}$ Torr was obtained. This resulted in attenuation of the ion beam by approximately 30%.

Kinetic energy release distributions were obtained from the shapes of the metastable peaks by using eq 2. $P(E)$ is the probability of a given

$$P(E) = dI/dE \qquad (2)$$

translational energy, and $dI/dE$ is the derivative of peak intensity with respect to energy.[18a,19] For $x$ = 3–6 metastables, the peaks were fitted to a polynomial before the derivative was taken, while for $x$ = 1 and 2 the unprocessed data were numerically differentiated. The effect of fitting the curve before differentiation is simply to smooth the resulting kinetic energy release distribution, with no quantitative effects on the results.

$Mn(CO)_5COCH_3$ and $Mn(CO)_5COCF_3$ were synthesized following published procedures.[20] The 99% purity of the $^{13}CO$ was verified by FTICR.

## Results

**CO Exchange Studies.** As an example of the results of the exchange experiments, signal intensities due to $Mn(CO)_{5-n}(^{13}CO)_n^+$, $n$ = 0–5 in the presence of $^{13}CO$, are shown as a function of time in Figure 1. Incorporation of the label into the metal carbonyl ion is clearly evident. The semilog plot of the unsubstituted $Mn(CO)_5^+$ signal versus time (Figure 2) is linear.

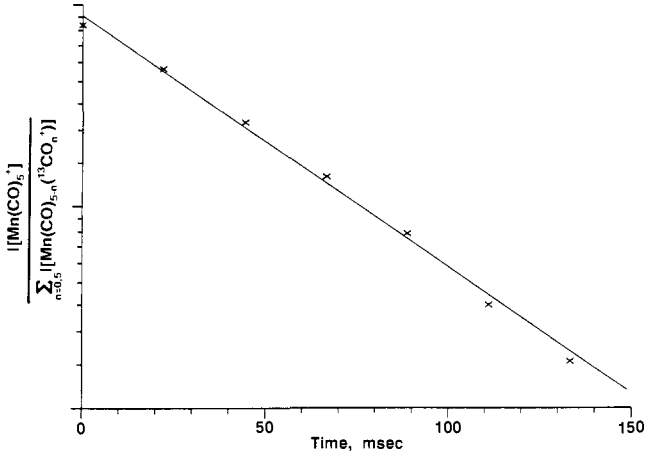


**Figure 2.** Plot of log $[I(Mn(CO)_5^+)/(\sum I(Mn(CO)_{5-n}(^{13}CO)_n^+))]$, $n$ = 0–5, versus time, using the data of Figure 1.

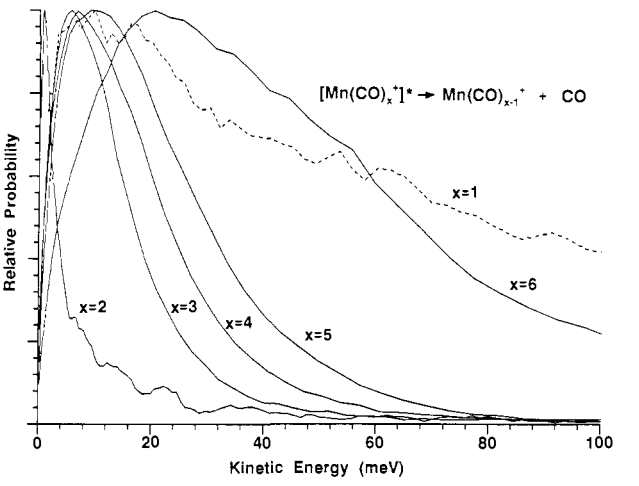


**Figure 3.** Kinetic energy release distributions for metastable $[Mn(CO)_x^+]^*$ decomposition. Data for $x$ = 1 (dashed line) reflect collision-induced dissociation rather than metastable decomposition.

**Table II.** CO Exchange Rates $Mn(CO)_x^+ + {}^{13}CO \rightarrow Mn(CO)_{x-1}{}^{13}CO^+ + CO$

| $x$ | $k^a$ | $k_{Langevin}{}^* x/(x+1)^a$ | efficiency, % |
|---|---|---|---|
| 6 | no reaction | 58 | 0 |
| 5 | 6.3 ± 0.7 | 57 | 11 |
| 4 | 4.8 ± 1.7 | 55 | 9 |
| 3 | 13.1 ± 3.3 | 52 | 25 |
| 2 | 17.5 ± 2.6 | 48 | 36 |
| 1 | 8.2 ± 1.8 | 37 | 22 |

[a] Units of $10^{-11}$ $cm^{-3}$ $molecule^{-1}$ $s^{-1}$.

Rate constants determined for reaction 3 are listed in Table II, along with reaction efficiencies calculated by dividing the measured rate constant by the Langevin collision rate, statistically adjusted for the number of CO's present (assuming all the ligands in the collision complex are equivalent). For $x$ = 1–5, the CO exchange rates are similar, with reaction efficiencies in the range 9–36%. No exchange is observed for $x$ = 6.

$$Mn(CO)_x^+ + {}^{13}CO \rightarrow [Mn(CO)_x{}^{13}CO]^+ \rightarrow Mn(CO)_{x-1}{}^{13}CO^+ + CO \qquad (3)$$

**Kinetic Energy Release Distributions.** In these experiments, metastable ions produced by electron impact fragmentation of the precursor dissociated in the second field-free region of the double-sector instrument according to reaction 4. Kinetic energy release distributions measured for the loss of CO from $Mn(CO)_x^+$

(19) For a discussion of the theory used in obtaining kinetic energy release distributions using metastable peak shapes, see: Jarrold, M. F.; Illies, A. J.; Kirchner, N. J.; Wagner-Redeker, W.; Bowers, M. T.; Mandich, M. L.; Beauchamp, J. L. *J. Phys. Chem.* **1983**, *87*, 2213–2221.

(20) Casey, C. P.; Scheck, D. M. *J. Am. Chem. Soc.* **1980**, *102*, 2728–2731.

($x$ = 2–6) metastables are plotted in Figure 3.

$$[Mn(CO)_x^+]^* \rightarrow Mn(CO)_{x-1}^+ + CO \quad (4)$$

The smaller metastable members of the $Mn(CO)_x^+$ series decompose quickly. Consequently, most decomposition occurs in the ion source rather than in the second field-free region, and metastables are therefore difficult to detect. For $x$ = 1, an added complication is the difficulty of distinguishing between metastable decomposition and CID resulting from collision with residual gas in the second field-free region. Examination of the variation in intensity of the $MnCO^+$ dissociation signal as the background pressure of He in the second field-free region was increased showed that for $MnCO^+$ the signal is primarily due to CID; it increases linearly with added He. The distribution obtained for $x$ = 2 is too narrow to be due to CID; distributions measured with He added to the collision cell are much broader. For $x > 2$, decomposition rates are slower, and this problem does not occur.

**Photodissociation Studies.** Kinetic energy release distributions were obtained for the photodissociation reactions (5). The details

$$Mn(CO)_x^+ + h\nu \rightarrow Mn(CO)_{x-2}^+ + 2CO \qquad x = 2, 5 \quad (5)$$

will be published elsewhere.[21] For both the $x$ = 2 and the $x$ = 5 cases the product kinetic energy distributions are peaked near zero and fall off essentially exponentially to higher energy. The average energies for the two systems are $\langle E_t(Mn(CO)_5^+)\rangle$ = 0.11 eV and $\langle E_t(Mn(CO)_2^+)\rangle$ = 0.29 eV, and the maximum kinetic energies are 0.42 ± 0.05 and 1.0 ± 0.1 eV for $Mn(CO)_5^+$ and $Mn(CO)_2^+$, respectively. Photodissociation of $MnCO^+$, as well as loss of a single CO from $Mn(CO)_2^+$, was not observed at 514 nm.

## Discussion

**Spin Conservation and CO Exchange Studies.** As was expected, no exchange was observed for $Mn(CO)_6^+$ since this is a stable, coordinatively saturated 18-electron ion and exchange would involve a crowded 20-electron intermediate. This same behavior is found in solution; at ambient temperature, no exchange of CO was observed for $Mn(CO)_6^+$ after 15 h.[22] Likewise, the isoelectronic $Cr(CO)_6$ is unreactive toward ligand exchange.[23]

If spin conservation is important in reactivity, then large variations in CO exchange rates are expected. It was therefore surprising to find that the CO exchange rates are similar for $x$ = 1–5. There was some small variation in exchange rates, but certainly the differences were much less than the 2.5 orders of magnitude observed for the neutral $Fe(CO)_x$ system.[2] Why $Fe(CO)_x$ and $Mn(CO)_x^+$ are so different warrants speculation.

One possibility is that $Mn(CO)_x^+$ compounds, $x$ = 1–6, all have singlet ground states and that the transition from septet to singlet takes place upon the addition of one CO. Comparison with the isoelectronic $Cr(CO)_x$ species yields some support for this idea: all CO addition reactions of $Cr(CO)_x$, $x$ = 2–5, were found to be rapid, leading to the prediction that all members of this series have singlet ground states.[5,24] However, it seems inconceivable that $MnCO^+$ has a singlet ground state: the lowest known singlet state of $Mn^+$ lies 4.8 eV above the septet ground state.[25] Assuming the existence of lower lying singlet $Mn^+$ states, the minimum energy required to produce a singlet from septet $Mn^+$ can be estimated to be at least 60 kcal/mol.[26] In either event, this is more energy than could reasonably be recovered through formation of the $Mn^+$–CO bond.

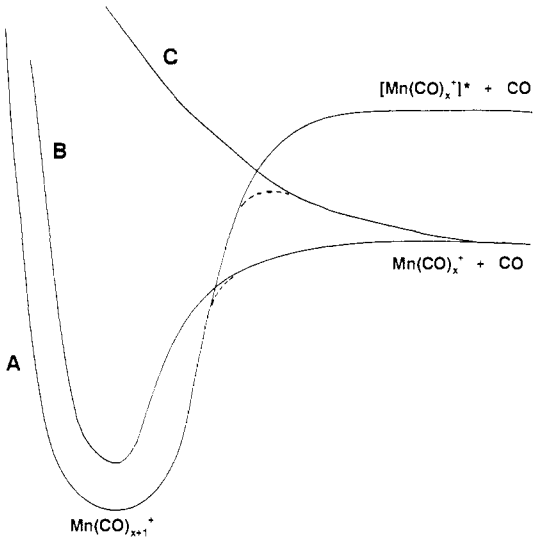


**Figure 4.** Schematic potential energy surfaces depicting crossings between attractive surfaces A and B and between attractive surface A and repulsive surface C. An exit channel barrier results in the latter case.

Another alternative is that the exchange reactions lead to excited products, conserving spin. This idea has several problems. It requires that the spins of the $Mn(CO)_x^+$ ground state, the $Mn(CO)_{x+1}^+$ complex leading to exchange, and the first $Mn(CO)_x^+$ excited state all be the same. Further, $Mn(CO)_{x+1}^+$ must dissociate to *excited* $Mn(CO)_x^+$, while being produced from ground-state $Mn(CO)_x^+$. This process is clearly endoergic and would not be expected to occur efficiently.

It is also possible that the reactants are in excited states. This is a common problem when using electron impact ionization.[27] While the possibility cannot be completely eliminated, several factors argue against it. The same results were obtained using $Mn(CO)_5COCH_3$ and $Mn(CO)_5COCF_3$ to generate the $Mn(CO)_x^+$. It seems improbable that both should lead to the same population of excited states. Further, the results showed no dependence on the 15–35-eV electron energy used for ionization. In addition, failure to observe metastable $MnCO^+$ implies that predissociation from a long-lived excited electronic state is not important in the $x$ = 1 case.[28] Finally, no curvature was apparent in any of the plots of log (signal intensity) versus time, arguing strongly that excited ions are absent. An example of such a plot, for the $x$ = 5 case, is given in Figure 2.

A more likely possibility is that the $Mn(CO)_x^+$ exchange reactions do not always probe the $Mn(CO)_{x+1}^+$ ground-state potential energy wells. For CO addition to neutral, coordinatively unsaturated metal carbonyls, the reactions occur at rates approximately 1 order of magnitude slower than collision-limited rates.[4,5] Similarly, the $Mn(CO)_x^+$ ions undergo CO exchange at only $^1/_3$–$^1/_{10}$ of the collision-limited rate. The relatively low efficiencies of the ion–molecule reactions argue that the incoming CO somehow remains unique in the major fractionof collisions. One situation where this might occur, illustrated in Figure 4, is when a crossing between two attractive surfaces (A and B in the figure) is involved. As CO approaches $Mn(CO)_x^+$ on surface B, the $Mn(CO)_{x+1}^+$ ground surface A is encountered. If the crossing occurs, the $Mn(CO)_{x+1}^+$ well is sampled and the uniqueness of the incoming CO is lost; exchange occurs when unlabeled CO is lost from the collision complex. If the crossing does not occur, the incoming CO remains unique and the collision does not result in exchange.

(21) van Koppen, P. A. M.; Bowers, M. T.; Dearden, D. V.; Beauchamp, J. L. To be submitted for publication.
(22) Hieber, W.; Wollmann, K. *Chem. Ber.* **1962**, *95*, 1552.
(23) Noted in a review: Werner, H. *Angew. Chem. Int. Ed. Engl.* **1968**, *7*, 930–941.
(24) (a) Seder, T.; Ouderkirk, A.; Church, S.; Weitz, E. In *High Energy Processes in Organometallic Chemistry*; Suslick, K. S., Ed.; American Chemical Society: Washington, DC, 1987. (b) Weitz, E. *J. Phys. Chem.* **1987**, *91*, 3945–3953.
(25) Sugar, J.; Corliss, C. *J. Phys. Chem. Ref. Data* **1985**, *14*, 351–363.
(26) This estimate is based on values calculated for $Mn^+$ in: Schilling, J. B. Ph.D. Thesis, California Institute of Technology, 1987. Assuming s–d exchange terms of 4 kcal/mol, conservatively estimating d–d exchange terms of 10 kcal/mol, and noting that formation of the singlet will cause the loss of at least 5 s–d and 4 d–d exchange terms, the total exchange energy lost in forming the singlet is 60 kcal/mol. This ignores the additional energetic cost of promoting the 4s electron to the 3d orbital.
(27) The excited-state population produced in surface ionization, electron impact, and drift cell ionization sources has recently been discussed: Sunderlin, L. S.; Armentrout, P. B. *J. Phys. Chem.* **1988**, *92*, 1209–1219.
(28) For an example of metastable electronic predissociation in $CrCO^+$ and $Cr(CO)_2^+$ see: Jarrold, M. F.; Misev, L.; Bowers, M. T. *J. Phys. Chem.* **1984**, *88*, 3928–3929.

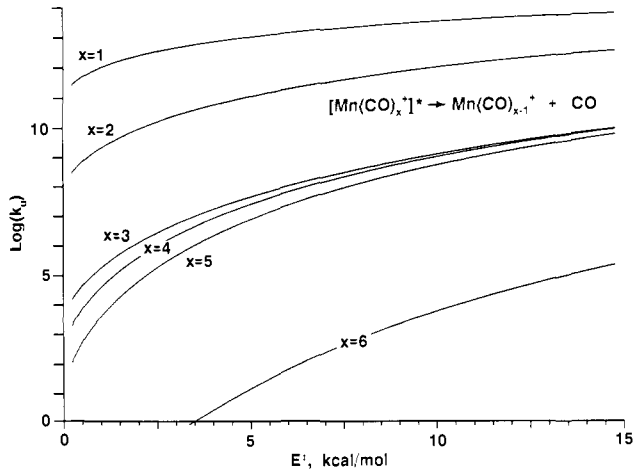


**Figure 5.** Unimolecular decomposition rate constants $k_u$ as a function of ion internal energy above threshold, $E^*$, calculated using RRKM theory employing Whitten–Rabinovitch state counting. Bond energies listed in Table III, with log $A$ = 15, were used in the calculations.

Alternatively, the low efficiencies may be explained more simply in terms of the requirements for geometric relaxation.[5] It is expected that some rearrangement of the bound ligands is generally required to accommodate the incoming, labeled ligand, and if a great deal of such relaxation is necessary, it is likely that the exchange process will be inefficient.

**Kinetic Energy Release Studies.** The CO exchange rate studies alone do not answer the question of the importance of spin conservation in the $Mn(CO)_x^+$ system. For further information we turn to the results of the kinetic energy release experiments.

These experiments are used to probe the nature of the potential surface in the exit channel. If CO loss is spin-forbidden it is possible a barrier exists in the exit channel. One possibility is illustrated in Figure 4, where the avoided crossing between the repulsive surface C and the ground-state surface A results in an exit channel barrier. Such a barrier should be detectable since it would almost certainly give rise to a nonstatistical kinetic energy release characterized by a broad distribution of energies shifted away from zero. In the absence of a barrier, a narrow distribution peaking near zero would be expected since the reaction coordinate in such a case is in statistical equilibrium with the other modes of the transition state.[15]

The trend in the widths of the kinetic energy release distributions, with $x$ = 6 giving the broadest and $x$ = 2 giving the narrowest (see Figure 3), at first seems counterintuitive: one might expect that the average energy released into translation should be largest for the smaller members of the series since these have the fewest degrees of freedom into which energy must be statistically partitioned. When the lifetime requirements for observation are considered, this apparent problem is resolved. Since metastable detection requires that dissociation take place in the second field-free region, the observed metastables must decompose approximately 5–20 $\mu$s after exiting the source. To have decomposition rates appropriate for observation, the larger members of the series must have considerably more excess energy than the smaller members, which have energies just above threshold. This is illustrated in Figure 5, where unimolecular decomposition rates calculated using RRKM theory are plotted as a function of internal energy. Even though the larger molecules have more modes among which energy must be partitioned, the larger excess energy they contain more than compensates, with the result being the noted trend. It is interesting to note that the kinetic energy release distributions for the photodissociation reactions,[21] with the lifetime requirements removed, have widths which follow the intuitive order: the larger molecule, with more modes among which to distribute the fixed amount of internal energy contributed by the 514-nm photon, produces the narrower distribution.

By using the method discussed below, it was possible to reproduce the kinetic energy release distributions for $x$ = 2–6 using phase space theory.[29-31] Details of the phase space calculations can be found in Appendices A and B. The metastable decompositions ($x$ = 2–6) could be described as statistical reactions on Type I surfaces; i.e. for $x$ = 2–6, there is no barrier to the reverse of reaction 4 since none of the energy distributions show the shift away from zero and broadening characteristic of nonstatistical energy releases.[15] Consequently, there is no barrier to the addition of CO to $Mn(CO)_x^+$, $x$ = 1–5, while the question of the presence of a barrier in the addition of CO to bare $Mn^+$ remains open.

These results are consistent in at least one case with theoretical calculations on isoelectronic species. For $Cr(CO)_5$ there is no barrier to CO addition.[32] Although the effects of surface crossings were not directly observed, the lack of barriers has implications about the type of surface crossings that might occur along the reaction coordinate as CO interacts with $Mn(CO)_x^+$. If crossings occur, they must be between *attractive* surfaces, since crossing with a repulsive surface would lead to a barrier in the resulting diabatic surface. This is illustrated in Figure 4, where the avoided crossing of attractive surfaces A and B results in a diabatic surface without an exit channel barrier, while the crossing of surface A and the repulsive surface C necessarily leads to a barrier.

Several recent theoretical calculations indicate that the bonding in first-row transition-metal monocarbonyl ions is qualitatively different from that of the corresponding neutrals. One study, employing GVB methods at the CI level,[33] suggests that the bonding in the ions is primarily electrostatic rather than the usual $\sigma$-donor $\pi$-acceptor picture envisioned for neutral metal carbonyls. If such were the case, the spin state of the metal center would not be expected to be important to the formation of an electrostatic bond. However, this idea only pushes the problem to a larger member of the series, since it is inconceivable that the bonding in $Mn(CO)_6^+$ is predominantly electrostatic; the low lability of the ligands as measured in the exchange experiment is inconsistent with bonding dominated by electrostatics and is in agreement with expectation for a closed-shell, 18-electron ion. Even if the electrostatic model is correct for small metal carbonyl ions, at some point as ligands are added, a more conventional bonding mode must come into play.

Another possibility is that spin transitions do occur as CO's are added, but that, in contrast to the neutral systems, spin conservation is relatively unimportant to the reaction dynamics. If crossings take place between attractive surfaces that are strongly coupled, no barrier would result in the exit channel and exchange rates would not be affected strongly. Or, if crossings take place at long range between narrowly separated surfaces, the result is the same. The experimental observations can also be explained if spin is not a good quantum number in the $Mn(CO)_x^+$ system. It seems reasonable that $d^6$ species, with the possibility of a large number of spin states further complicated by spin–orbit interactions, might exhibit a great deal of mixing of different spin states. Further experimental and theoretical work is needed to resolve the question. High-level calculations to determine the ground states and structures of the $Mn(CO)_x^+$ ions would be especially illuminating.

**Extraction of Bond Energies from Kinetic Energy Release Data.** According to the phase space description, the statistical kinetic energy release distribution is a strong function of the amount of energy above threshold in the energized molecule,[15] $E^*$, which in the dissociation of $Mn(CO)_x^+$ metastables is just the difference between $\Delta H$ and $E^*$, the internal energy of the metastable. Other parameters (see Appendix A) are required for phase space calculation of kinetic energy release distributions, but these are either well-known or easily estimated and generally do not have a strong effect on the calculated distribution. When $E^*$ is known and the

(29) For discussion of the application of phase space theory to the fitting of kinetic energy release distributions, see: (a) Chesnavich, W. J.; Bowers, M. T. *J. Am. Chem. Soc.* **1977**, *99*, 1705–1711. (b) Jarrold, M. F.; Wagner-Redeker, W.; Illies, A. J.; Kirchner, N. J.; Bowers, M. T. *Int. J. Mass Spectrom. Ion Proc.* **1984**, *58*, 63–95. (c) Reference 30.

(30) Chesnavich, W. J.; Bass, L.; Su, T.; Bowers, M. T. *J. Chem. Phys.* **1981**, *74*, 2228–2246.

(31) Chesnavich, W. J.; Bowers, M. T. *Prog. React. Kinet.* **1982**, *11*, 137.

(32) Sherwood, D. E., Jr.; Hall, M. B. *Inorg. Chem.* **1983**, *22*, 93–100.

(33) Allison, J.; Mavridis, A.; Harrison, J. F. *Polyhedron*, in press.

kinetic energy release is statistical, $\Delta H$ for the decomposition can be derived by fitting the experimental data with the theoretical energy release predicted by phase space theory.[15,34] The technique has until now been limited by the requirement that $E^*$ be well-defined. In this section it will be shown that quantitative results can also be extracted when the ions have a *broad range* of internal excitation, since the experiment places severe constraints on the values of $E^*$ which contribute to the measured distribution.

The $Mn(CO)_x^+$ system is an example of the situation just mentioned. The ions were all produced by electron impact followed by fragmentation, with the result that the internal energies of the metastables were unknown. This difficulty was circumvented by taking note that the lifetime requirements for the observation of metastables are stringent: the metastables must decompose during the time they are in the second field-free region, a window of approximately 5–20 $\mu$s after extraction from the source. The lifetime requirement in turn places limitations on $E^*$. If $E^*$ is too large, most metastable decomposition occurs before the ions reach the second field-free region and the resulting signal is weak. If $E^*$ is too small, most metastables will decompose after transiting the second field-free region and again the signal is weak. These limitations can be quantified using statistical kinetic theory to determine decomposition rates as a function of ion internal energy. The energies are then assigned weights $W(E^*)$ according to eq 6 using theoretically determined rate constants for unimolecular

$$W(E^*) = \exp[-k_u(E^*)(t_i + t_r)] - \exp[-k_u(E^*)(t_f + t_r)] \quad (6)$$

decomposition, $k_u(E^*)$. The transit times from the source to the entrance and exit of the second field-free region are given by $t_i$ and $t_i$, respectively, while $t_r$ is the residence time of the ion in the source between formation and extraction. In this work $t_r = 0$ was assumed, since over a reasonable range of residence times the results do not depend strongly on $t_r$.

RRKM theory[35] was employed to determine the unimolecular rate constants. This takes advantage of the observation that dissociation rates are best described using tight transition states, even though the release of energy into product separation is best described by an orbiting transition state.[36,37] The results have a strong dependence onthe tightness of the RRKM transition state chosen, which in turn is quantitatively reflected by the size of the frequency factor (hereafter denoted $A$-factor). To our knowledge experimental $A$-factors for loss of CO from $Mn(CO)_x^+$ have not been determined, so several means were used to estimate the values. First, comparison was made with a study[38] of the $A$-factors for CO loss from the neutrals $Fe(CO)_5$, $Cr(CO)_6$, $Mo(CO)_6$, and $W(CO)_6$. log $A$ was found to be in the range 15.5–16.0 for those species. This should serve as an upper limit for ionic $Mn(CO)_6^+$, where log $A$ might be expected to be lower because the charge-induced dipole interaction causes the transition state to be tighter in the ion than in the neutral case. Second, eq 7 may be used

$$A = (ekT/h)\exp(\Delta S^{\ddagger}/R) \quad (7)$$

to estimate $A$.[39] If it is assumed that the transition state is tight

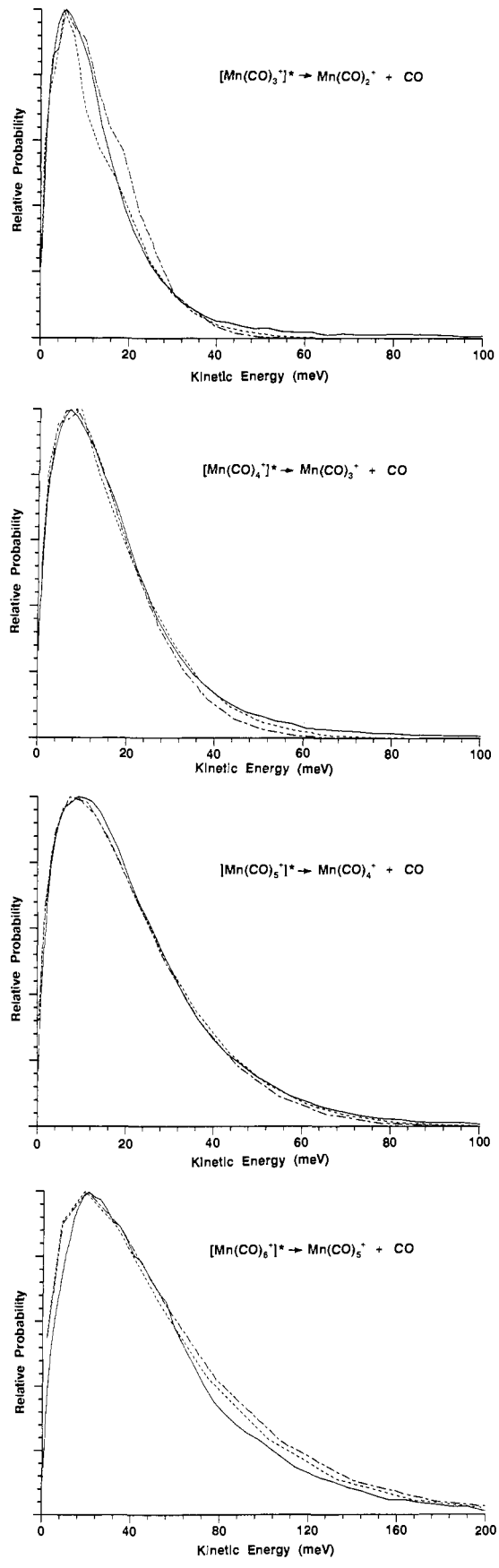


**Figure 6.** Comparison of theoretical kinetic energy release distributions to experimental distributions, obtained using the approach described in the text: experiment, solid line; theory at low log $A$ limit, short dashed line; theory at high log $A$ limit, long-short dashed line. Theoretical fits correspond to parameters given in Table III. Note change of scale for $x = 6$.

(34) van Koppen, P. A. M.; Jacobsen, D. B.; Illies, A. J.; Bowers, M. T.; Hanratty, M. A.; Beauchamp, J. L., submitted for publication in *J. Am. Chem. Soc.*

(35) Robinson, J. P.; Holbrook, K. A. *Unimolecular Reactions*; Wiley-Interscience: New York, 1972. Forst, W. *Theory of Unimolecular Reactions*; Academic Press: New York, 1973.

(36) This is another way of saying that metastable lifetimes are determined by the tight transition state but that the reaction coordinate remains coupled to the internal modes as products separate to the orbiting transition state and dissociate. See ref 30.

(37) RRKM theory can also be used, with the RRKM transition state, to calculate product kinetic energy release. This was done for the $x = 5$ case. Since it ignores the constraints imposed by angular momentum, the RRKM calculation fails to predict the dropoff in the distribution as kinetic energy approaches zero but does reasonably well in fitting the higher energy portion of the experimental distribution, with bond energies within the range calculated using phase space theory.

(38) Lewis, K. E.; Golden, D. M.; Smith, G. P. *J. Am. Chem. Soc.* **1984**, *106*, 3905–3912.

(39) Benson, S. W. *Thermochemical Kinetics*, 2nd ed.; Wiley-Interscience: New York, 1976.

**Table III.** Metastable Kinetic Energy Releases and $Mn(CO)_x^+$ Bond Energies

| $x$ | $(E_t)^a$ | $s^b$ | log $A^c$ | $E^*_{max}{}^d$ | $D_0^0(Mn(CO)_{x-1}^+-CO)^e$ |
|---|---|---|---|---|---|
| 6 | 55 | 33 | 15.0 | 50.0 | 37.0 |
| | | | 13.0 | 40.0 | 27.0 |
| 5 | 24 | 27 | 15.0 | 21.2 | 19.0 |
| | | | 13.0 | 15.3 | 13.0 |
| 4 | 19 | 21 | 15.3 | 24.2 | 23.0 |
| | | | 13.0 | 18.1 | 17.0 |
| 3 | 16 | 15 | 15.4 | 37.7 | 37.0 |
| | | | 13.0 | 26.0 | 25.0 |
| 2 | 11 | 10 | *f* | *f* | <25.0 |
| 1 | g | 4 | *f* | *f* | >7.0 |

[a] Measured average translational energy release in metastable decomposition in millielectronvolts. [b] Number of vibrational oscillators in $Mn(CO)_x^+$. [c] Frequency factor assumed for calculation of metastable internal energy. [d] Determined using eq 6 from text. Units in kilocalories per mole. [e] See text. Units in kilocalories per mole. [f] Fit not achieved. See text. [g] Not determined. See text.

(i.e. similar to the reactant), then $\Delta S$ is small and can be ignored except for a statistical factor deriving from the reaction path degeneracy. At 350 K using a path degeneracy of 6, eq 7 gives $\log A = 14.1$ for CO loss from $Mn(CO)_6^+$. This is also consistent with a careful choice of vibrational frequencies based on reasonable assumptions about the transition state (see Appendix A). We conclude that $\log A$ for $Mn(CO)_6^+$ decomposition is somewhere in the range 13–15.5 and fit the kinetic energy releases by varying $\Delta H$ at each of these extremes. The resulting bond energies, given in Table III, are bracketed accordingly. Details of the procedures used in obtaining the fits are given in Appendix B.

Examples of the fits obtained for the kinetic energy release distributions in reaction 4, $x = 2$–6, are given in Figure 6. The distributions for the larger values of $x$ were easily reproduced by the theory, but for $x < 4$ the quality of the fit deteriorates markedly as $x$ decreases. For $x = 2$, the experimental data could not be fit within the bounds of the $A$-factor discussed above. This may reflect the fact that the larger molecules, with greater internal energy and more modes into which it may be partitioned, are better described using statistical theory than are the smaller molecules, where quantum effects and other types of nonstatistical behavior are likely to be more important. It may also indicate a shortcoming in the method used to generate the limits on the $A$-factors.[40]

**Bond Energies.** If values of $E^*$ weighted as described above are used in the phase space calculations and $\Delta H$ is varied until a good fit between the phase space prediction and the experimental kinetic energy release is obtained, the bond energies listed in Table III are derived. Only an upper limit is reported for $D(MnCo^+-CO)$ since, as noted above, a good fit to the $Mn(CO)_2^+$ dissociation data could not be obtained.

Although the individual bond energies have not been measured by other means, the values given here may be compared with averages reported elsewhere. A recent ab initio study obtained a mean intrinsic bond energy of 32 kcal/mol in $Mn(CO)_6^+$ to the lowest singlet state of $Mn^+$ arising from a $d^6$ configuration, in which the $t_{2g}$ orbitals are fully populated.[41] If $^1/_6$ of the promotion energy required to produce the lowest known singlet state of $Mn^+$ is subtracted from this value, the results is 14 kcal/mol. This is considerably less than the 25 kcal/mol average of the measured values for $D(Mn(CO)_5^+-CO)$, $D(Mn(CO)_4^+-CO)$, $D(Mn(CO)_3^+-CO)$, and $D(Mn(CO)_2^+-CO)$ from Table III, but the theoretical results were also low by comparison to experiment for Cr, Mo, and W hexacarbonyls.

Further comparisons come from experimental results, and the agreement found is good. Since $\Delta H_f^\circ(Mn(CO)_5^+)$ is known,[11] $\Delta H$ can be calculated for reaction 8. $\Delta H$ for this reaction, 99

$$Mn(CO)_5^+ \rightarrow Mn^+ + 5CO \qquad (8)$$

kcal/mol, is the sum of all the $Mn^+$–CO bond energies in $Mn(CO)_5^+$, so the average $Mn^+$–CO bond energy is 19.8 kcal/mol. This agrees well with the average of $D(Mn(CO)_4^+-CO)$, $D(Mn(CO)_3^+-CO)$, and $D(Mn(CO)_2^+-CO)$ from Table III, 22 kcal/mol. More recently, the loss of two carbonyls from $Mn(CO)_5^+$ was studied by photodissociation threshold measurements, and the average of those two bond energies was determined to be <21.9 kcal/mol,[42] again in good agreement with the average from Table III, 18 kcal/mol.

Finally, the photodissociation study of reaction 5 gives an upper limit to the sum of $D(MnCO^+-CO)$ and $D(Mn^+-CO)$. From energy conservation, the relation of eq 9 is derived. $E_{int}(X)$ is the

$$D_0^0(MnCO^+-CO) + D_0^0(Mn^+-CO) = h\nu + E_{int}(Mn(CO)_2^+) - E_{int}(CO) - E_{int}(Mn^+) - E_t \qquad (9)$$

internal energy of X, and $E_t$ is the translational energy of the photofragments. The value of $E_{int}(CO)$ will be small due to the widely spaced vibrational levels in CO, and $E_{int}(Mn^+)$ is zero since the first excited state of $Mn^+$ is 1.17 eV above the ground state. A very small fraction of the $Mn(CO)_2^+$ ions will have enough energy to dissociate ($\sim 10^{-5}$), but the average internal energy in $Mn(CO)_2^+$ will be small (of the order of 2 ± 2 kcal/mol). Consequently, (9) can be simplified to (10). $E_t(max)$ is the

$$D_0^0(MnCO^+-CO) + D_0^0(Mn^+-CO) \approx h\nu - E_t(max) \qquad (10)$$

maximum kinetic energy released in the photofragmentation. The value so obtained, 32 ± 3 kcal/mol, is in excellent agreement with the 32 kcal/mol difference between $\Delta H$ for reaction 8 and the sum of our determined bond energies. In summary, in every case the values obtained by fitting the data using phase space theory agree with experimental values measured by independent methods. This lends support to the values of the various bond energies we have determined (Table II).

Few theoretically determined bond energies are available for comparison with the values reported here for the $Mn(CO)_x^+$ series. The value for $D(Mn(CO)_5^+-CO)$ obtained in the present work is intermediate between a value of 22 kcal/mol obtained using density functional theory[41] and the 49.6 kcal/mol obtained by modified extended Hückel calculations.[43] The density functional results, however, were low relative to a number of experimental values reported for $D(Cr(CO)_5-CO)$, $D(Mo(CO)_5-CO)$, and $D(W(CO)_5-CO)$, while the extended Hückel value might be expected to be high; the same calculation yielded 59 kcal/mol as the threshold for CO loss from the isoelectronic $Cr(CO)_6$, while photoacoustic calorimetry measurements gave 37 ± 5 kcal/mol for the same bond.[44] The reason for the discrepancy is unknown. Hartree–Fock calculations for $D(Cr(CO)_5^+-CO)$ also resulted in a higher value, 49.8 kcal/mol.[32] For the coordinatively unsaturated fragments, less information is available. The modified extended Hückel calculations noted above give 46.4 kcal/mol for $D(Mn(CO)_4^+-CO)$, in poor agreement with the current result of 16 ± 3 kcal/mol. These calculations are expected to do poorly in cases where spin is not conserved,[43] as may be the case here.

The variation in bond energies among the members of the $Mn(CO)_x^+$ series is not unique. As noted in Table IV, large variations in bond energies among members of $M(CO)_x$ series have previously been reported for iron[8] and nickel.[9] Appearance potential measurements have yielded a similar result for $Cr(CO)_x^+$ and $Mn(CO)_xBz^+$ (Bz = $CH_2C_6H_5$) ions.[10,11] The similarity in

(40) The concept of "preexponential" or "Arrhenius" $A$-factor is only strictly valid for systems in thermal equilibrium. Such systems generate canonical ensembles of energy states. In our electron impact generated $Mn(CO)_x^+$ ions, we have a microcanonical ensemble of energy states that depends on the energy deposition function for the initial ionization step and the energy partitioning as sequential CO ligands are lost. Hence, the method used here only semiquantitatively mimics the real situation. Since the $A$-factors are used only to set limits on the bond energies, the procedure is probably satisfactory.

(41) Ziegler, T.; Tschinke, V.; Ursenbach, C. *J. Am. Chem. Soc.* **1987**, *109*, 4825–4837.

(42) Tecklenburg, R. E., Jr.; Russell, D. H. *J. Am. Chem. Soc.* **1987**, *109*, 7654–7662.

(43) McKinney, R. J.; Pensak, D. A. *Inorg. Chem.* **1979**, *18*, 3413–3417.

(44) Bernstein, M.; Simon, J. D.; Peters, K. S. *Chem. Phys. Lett.* **1983**, *100*, 241–244.

**Table IV.** Bond Energies in Metal Carbonyls

| bond | species M | | | | | |
|---|---|---|---|---|---|---|
| | $Mn^+$ [a] | Cr [b] | $Cr^+$ [c] | $MnBz^+$ [d] | Fe [e] | Ni [f] |
| $M(CO)_5$–CO | 32 ± 5 | 37 ± 5 | 33 | | | |
| $M(CO)_4$–CO | 16 ± 3 | 25 ± 5 | 14 | 10 | 55 ± 11 | |
| $M(CO)_3$–CO | 20 ± 3 | | 21 | 21 | 5 ± 5 | 25 ± 2 |
| $M(CO)_2$–CO | 31 ± 6 | | 28 | 12 | 32 ± 7 | 13 ± 10 |
| $M(CO)_1$–CO | <25 | | 35 | 25 | 23 ± 7 | 54 ± 15 |
| M–CO | >7 | | 31 [g] | 30 | 21 ± 7 | 29 ± 15 |

[a] This work. [b] Reference 4c. [c] Reference 10. [d] Reference 11. [e] Reference 8. [f] Reference 9. [g] A more recent experimental result gives 26 ± 5 kcal/mol for this bond energy: Georgiadis, R.; Armentrout, P. B. submitted for publication in *J. Mass Spectrom. Ion Proc.* In addition, theoretical calculations at the CI level suggest a somewhat lower value of 15 kcal/mol.[33]

the bond strengths for $Mn(CO)_x^+$ and $Cr(CO)_x^+$, $x$ = 3–6, is striking.

Several things are apparent from the trends in bond energies. The $Mn(CO)_6^+$ ion exhibits special stability, as is evident from the large value of $D(Mn(CO)_5^+–CO)$. This seems reasonable since $Mn(CO)_6^+$ is an octahedral species[45] with all six valence electrons singlet paired in the $t_{2g}$ orbitals. Formation of the last $Mn^+$–CO bond results in a coordinatively saturated species. A similar situation exists for $D(Fe(CO)_4–CO)$, where the energy of this bond, at 55 kcal/mol, is the largest of the $Fe(CO)_x$ series.[8]

$D(Mn(CO)_5^+–CO)$ is weaker than the measured bond energies for group VI neutral hexacarbonyls in solution (Cr, 37 ± 5; Mo, 34 ± 5; and W, 38 ± 5 kcal/mol)[44] and in the gas phase (Cr, 37 ± 5 kcal/mol),[4c] since in the ion the $\pi$-bonding interactions are weakened relative to those of the neutrals. The same observation can be made when $D(M(CO)_4–CO)$ values for M = $Mn^+$ (16 ± 3 kcal/mol) and M = Cr (25 ± 5 kcal/mol) are compared.[4c] For ions, one might expect $\sigma$-bonding to be more important in relation to $\pi$-interactions than in corresponding neutrals, since the charge on the metal should stabilize $\sigma$-donation and decrease the amount of $\pi$-back-donation. High-level theory supports intuition. Ab initio calculations on $NiCO^+$ using a double-$\zeta$ basis at the SCF and MCSCF levels[46] found that, in contrast to the corresponding neutral NiCO, the ion has little $\pi$-bonding. Similar results were obtained in Hartree–Fock calculations on $CuCO^+$ using a large, polarized basis set at the SCF and MP4 levels.[47] It is expected that the relative importance of the $\pi$-interactions might increase as ligands are added to the metal and the ability to delocalize the charge increases, but even for $Mn(CO)_6^+$ theory predicts that back-bonding is less important than in the isoelectronic $Cr(CO)_6$ due to the charge on the metal center.[41]

For the smaller fragment ions, the relationship between their relative stabilities and their structures is difficult to characterize because of limited structural information.

For $MnCO^+$, the bonding is expected to be weak since formation of the bond would require promotion of the 4s electron to a d orbital. The lowest known state arising from a $d^6$ configuration of the $Mn^+$ ion ($^5D$) lies 41 kcal/mol above the ground state.[25] It is interesting to note the evidence from Table IV that $Cr^+$, having a ground state deriving from a $d^5$ configuration which lacks the 4s electron, forms a strong bond to CO. The data indicate that $MnCO^+$ is bound by >7 kcal/mol, in contrast to MnCO where analysis of matrix IR data indicates that the neutral is not bound.[48] The fact that absorption of 514-nm light results exclusively in loss of both CO's from $Mn(CO)_2^+$ argues that $D(Mn^+–CO)$ is weak. The matrix isolation data also support that conclusion. Of the measured CO stretching frequencies in first-row transition-metal monocarbonyl neutrals, only those of NiCO and CuCO are higher than that for CrCO, indicating a weak Cr–CO bond. Since $Mn^+$–CO is isoelectronic with CrCO, a weak $Mn^+$–CO bond is suggested.

(45) Modified extended Hückel calculations were performed for $Mn(CO)_6^+$, $Mn(CO)_5^+$, and $Mn(CO)_4$: Pensak, D. A.; McKinney, R. J. *Inorg. Chem.* **1979**, *18*, 3407–3413.

(46) Bauschlicher, C. W., Jr.; Bagus, P. S.; Nelin, C. J. Roos, B. O. *J. Chem. Phys.* **1986**, *85*, 354–364.

(47) Morgantini, P.-Y.; Weber, J., to be published in *THEOCHEM*.

(48) Bach, S. B. H.; Taylor, C. A.; Van Zee, R. J.; Vala, M. T.; Weltner, W., Jr. *J. Am. Chem. Soc.* **1986**, *108*, 7104–7105.

## Summary

Many questions remain concerning the influence of spin conservation on the reactivity and bonding of metal carbonyls, but it is clear that spin is less important in the $Mn(CO)_x^+$ system than in the neutral $Fe(CO)_x$ system. While changes in spin multiplicity must occur as CO ligands are successively added to $Mn^+$, their effects are not manifested in terms of CO exchange rates or barriers in the exit channel for CO loss. The reasons for this behavior are unclear but may lie in the differences in the bonding of neutral metal atoms and ionic metal centers to CO as suggested by ab initio calculations. In addition, it is likely that the $d^6$ $Mn(CO)_x^+$ system is electronically more complex than the $d^8$ $Fe(CO)_x$ system, with the result than spin is a poorer quantum number for the $Mn(CO)_x^+$ ions.

Useful thermochemical information can be extracted by modeling kinetic energy release distributions using statistical dynamic theories. This technique should be generally applicable to metastable ions which decompose with no barrier to the reverse association reaction. It is not necessary to take special care that the internal energy of the metastable be well-defined; energy selection is built into the experiment by the requirement that decomposition occurs during a narrow time window. A further advantage is that, unlike many physical methods for measuring thermochemistry, this method works best with relatively large molecules, where the statistical description of energy transfer is most accurate due to high state densities. In addition, the average kinetic energy release is larger (and therefore easier to measure), since larger ion internal energies are necessary to achieve optimum decomposition rates than for smaller molecules.

The application of these techniques to the $Mn(CO)_x^+$ system has resulted in measurements of a number of metal carbonyl bond energies for this system, which are in agreement with average bond energies measured using other methods. The bonding trends can be rationalized in terms of simple molecular orbital arguments, with the bonding in the ions being simpler than that in the corresponding neutrals due to the relative unimportance of $\pi$-bonding in the ions. The reasons for the differences in the importance of spin in the neutral metal carbonyls and the $Mn(CO)_x^+$ system are unclear and warrant further investigation.

**Acknowledgment.** This work has been funded by the National Science Foundation through Grant No. CHE87-11567 (J.L.B.) and CHE85-12711 (M.T.B.) and graduate fellowship support (D.V.D.). In addition, we thank the Shell Foundation for graduate fellowship funding (D.V.D.) and the donors of the Petroleum Research Fund, administered by the American Chemical Society, for additional support. The help of Tim Swager in synthesizing $Mn(CO)_5COCH_3$ is also appreciated, and we thank John Bercaw for providing $^{13}CO$ for use in the exchange experiments.

## Appendix A: Parameters for Statistical Calculations

Fundamental vibrational frequencies for $Mn(CO)_6^+$ have been assigned based on infrared and Raman spectra of $Mn(CO)_6^+$-$PF_6^-$,[49] and these frequencies were used to estimate those of the gas-phase ions. In general, the frequencies were adjusted to produced the desired $A$-factor. It should be noted that the results have only a weak dependence on the frequencies chosen, as long

(49) McLean, R. A. N. *Can. J. Chem.* **1974**, *52*, 213–215.

as the $A$-factor remains constant.

Structures for the various $Mn(CO)_x^+$ ions were assumed as noted. $Mn(CO)_6^+$ was assumed to be an octahedral complex with Mn-C bond lengths of 1.87 Å and C-O bond lengths of 1.14 Å.

Two possibilities are considered for $Mn(CO)_5^+$: a $C_{4v}$ structure resulting from removal of one CO ligand from octahedral $Mn(CO)_6^+$ and a rearranged trigonal-bipyramidal structure. The $C_{4v}$ geometry has been predicted by Burdett for a singlet $d^6$ metal pentacarbonyl.[14] Further support for the $C_{4v}$ geometry comes from X-ray crystallographic data[50] and gas-phase electron diffraction data[51] for $HMn(CO)_5$, as well as modified extended Hückel calculations[45] on $Mn(CO)_5^+$. Bond lengths were taken from theory.[45] The isoelectronic $Cr(CO)_5^+$ has also been determined to have $C_{4v}$ geometry on the basis of its infrared spectrum.[52] $Fe(CO)_5^+$, on the other hand, is believed to be trigonal bipyramidal.[14]

For $Mn(CO)_4^+$, $C_{2v}$, $D_{4h}$, and $T_d$ geometries were considered. It has been predicted that singlet $d^6$ tetracarbonyls should have the $C_{2v}$ geometry.[14] Infrared spectra[53] and CO addition rates[4,5] for the isoelectronic $Cr(CO)_4$ indicated that this molecule has a $C_{2v}$ ground state, while modified extended Hückel calculations[54] on neutral $Mn(CO)_4$ also predict this structure. Calculated bond lengths were used.[45] Burdett argues, on the basis of theory, that quintet $d^6$ metal tetracarbonyls should have the $T_d$ structure.[14]

Three geometric possibilities, $C_{3v}$, $D_{3h}$, and $C_{2v}$, are considered for $Mn(CO)_3^+$. Burdett has predicted that the $C_{3v}$ $d^6$ metal tricarbonyl has a singlet ground state, while the $C_{2v}$ geometry results in a triplet and the $D_{3h}$ geometry is a quintet. Infrared spectral data[53] for the isoelectronic neutrals $Mo(CO)_3$ and $Cr(CO)_3$ are consistent with $C_{3v}$ geometry for both species. Bond lengths were assumed: Mn-C, 1.84 Å; C-O, 1.15 Å.

### Appendix B: Method of Calculation

Fits of theoretical kinetic energy release distributions to the measured experimental distributions were obtained as follows. Initially, a guess was made for the bond energy in question, and this value was used to estimate metastable internal energies assuming the low extreme for log $A$ as discussed above. Decomposition rate constants were calculated using RRKM theory,[55] with the assumed bond energy and log $A$, for a range of ion internal energies. The internal energies were then assigned weights by using the calculated rate constants in eq 6, and phase space calculations[56] were performed using the weighted internal energies. The same bond energy was used in the phase space calculation as was assumed for the RRKM calculation. On the basis of the comparison of the calculated kinetic energy distribution to the experimental distribution, the bond energy was revised and the process was repeated with a new RRKM calculation. This iteration was continued until the bond energy was bracketed for the low log $A$ value, generally to ±0.5 kcal/mol. At that point the high value for log $A$ was assumed, a new guess was made for the bond energy, and iterations were performed until the fit converged on a bond energy at the high log $A$ value. It is important to note that RRKM theory was used only to determine the metastable internal energies; otherwise, the phase space calculations and fitting procedures did not depend on the RRKM calculations.

(50) La Placa, S. J.; Hamilton, W. C.; Ibers, J. A. *Inorg. Chem.* **1964**, *3*, 1491-1495.
(51) Robiette, A. G.; Sheldrick, G. M.; Simpson, R. N. F. *J. Mol. Struct.* **1969**, *4*, 221-231.
(52) Huber, H.; Kundig, E. P.; Ozin, G. A.; Poe, A. J. *J. Am. Chem. Soc.* **1975**, *97*, 308-314.
(53) Perutz, R. N.; Turner, J. J. *J. Am. Chem. Soc.* **1975**, *97*, 4800-4804.
(54) Elian, M.; Hoffmann, R. *Inorg. Chem.* **1975**, *14*, 1058-1076. Also see ref 45.
(55) RRKM calculations were performed using: Hase, W. L.; Bunker, D. L. *A General RRKM Program.* Grouped harmonic frequency direct counting was used to determine sums and densities of states in the activated complexes, while the Whitten-Rabinovitch approximation[35] was used for energized molecules.
(56) A more recent version of the phase space programs used has been submitted to QCPE: Chesnavich, W. J.; Bass, L.; Grice, M. E.; Song, K.; Webb, D. A. TSTPST: Statistical Theory Package for RRKM/QET/TST/PST Calculations *QCPE*, submitted for publication.

# Interaction of Triplet Sensitizers with Chlorophyll: Formation of Singlet Chlorophyll[1]

**Cornelia Bohne[2] and J. C. Scaiano***

*Contribution from the Division of Chemistry, National Research Council of Canada, Ottawa, Ontario, Canada K1A OR6.* *Received August 9, 1988*

**Abstract:** The interaction of several triplet sensitizers with chlorophyll *a* (Chl*a*) has been examined using laser techniques. For the carbonyl sensitizers (with triplet energies >53 kcal/mol) it was possible to measure the quenching rate constants; these were systematically $\geq 10^{10}$ $M^{-1}$ $s^{-1}$. In the cases of acetone, benzophenone, and *p*-methoxyacetophenone the quenching process leads to the formation of the fluorescent singlet state of Chl*a*. For benzophenone ($k_q = 2.4 \times 10^{10}$ $M^{-1}$ $s^{-1}$) approximately 3% of the quenching events lead to the formation of excited Chl*a*. Several sensitizers (decafluorobenzophenone, benzil, and fluorenone) do not induce Chl*a* fluorescence (or do it very inefficiently) in spite of having triplet energies above the $S_1$ level of Chl*a*. In light of our results the most probable mechanism involves energy transfer from the triplet sensitizer to an upper triplet state of Chl*a* ($^3$Chl*a*$^{**}$) which can undergo reverse intersystem crossing to the singlet manifold of Chl*a* and thus induce fluorescence. The inefficient sensitizers are those where electron transfer between the excited singlet of Chl*a* or $^3$Chl*a*$^{**}$ and ground-state sensitizers is energetically favorable, leading to rapid in-cage quenching of the initially formed excited states of Chl*a*. Formation of radical-ion pair between the triplet sensitizer and Chl*a* followed by the generation of singlet Chl*a* in the recombination of the radical ions could not be completely discarded.

Chlorophyll *a* (Chl*a*) fluorescence can be induced by enzymatically generated triplet carbonyl compounds. This process has been observed for Chl*a* in various media, such as aqueous or micellar solutions, when part of chloroplasts or thylakoid fractions, and when bound to serum albumins.[3,4] Two possible mechanisms were suggested: (i) triplet-triplet energy transfer to an upper triplet of Chl*a* and a subsequent population of its $S_1$ state by reverse intersystem crossing (RISC),[3] or (ii) radical-ion pair formation between the triplet sensitizer and Chl*a* followed by

(1) Issued as NRCC-29983.
(2) Postdoctoral Fellow from the Conselho Nacional de Desenvolvimento Cientifico e Tecnologico ($CNP_q$), Brazil.
(3) Bohne, C.; Campa, A.; Cilento, G.; Nassi, L.; Villablanca, M. *Anal. Biochem.* **1986**, *155*, 1.
(4) Bohne, C.; Faljoni-Alario, A.; Cilento, G. *Photochem. Photobiol.* **1988**, *48*, 341.

0002-7863/89/1511-2409$01.50/0 Published 1989 by the American Chemical Society